Inorganica Chimica Acta 427 (2015) 41–51

Contents lists available at ScienceDirect

Inorganica Chimica Acta

journal homepage: www.elsevier.com/locate/ica

Structural elucidation of a few electron-deficient porphyrin/fullerene cocrystallates: Effect of fullerene on the porphyrin ring conformation

K. Karunanithi, P. Bhyrappa *

Department of Chemistry, Indian Institute of Technology Madras, Chennai 600 036, India

ARTICLE INFO

Article history:
Received 1 July 2014
Received in revised form 23 October 2014
Accepted 5 December 2014
Available online 15 December 2014

Keywords:
Crystal structures
Nonplanar porphyrins
Metalloporphyrins
Porphyrin/fullerene cocrystallates
Supramolecular chemistry

ABSTRACT

A series of electron-deficient porphyrin/fullerene solvated cocrystallates, β-tetracyano/tetrabromo-*meso*-tetraphenylporphyrin/C_n (n = 60 or 70) [$(H_2TPP(CN)_4)_3{\cdot}C_{60}$, **1**; $(CuTPP(CN)_4)_3{\cdot}C_{60}$, **2**; $(H_2TPP(CN)_4){\cdot}C_{70}$, **3**; $(H_2TPPBr_4){\cdot}(C_{60})_2$, **4**] were examined by single crystal XRD analysis. Cocrystallates **1** and **2** showed hexagonal honeycomb layer-like structure while **3** and **4** revealed one-dimensional linear/zigzag chain structure. Porphyrin ring in the cocrystallates, **1**–**3** revealed enhanced distortion (r.m.s. > 0.245(6) Å) than that of a nearly planar parent $H_2TPP(CN)_4$ (0.046(3) Å) structure. The supramolecular interactions in the cocrystallates, **1**–**4** revealed shortest (por)C...C(C_{70}) = 3.165 Å, (C_{60})C...N_{por} = 3.034 Å and (C_{60})C...C(C_{60}) = 2.992 Å close contact distances. The normal-coordinate structural decomposition analysis of the macrocycle in **1**–**3** revealed mainly *saddling* (~71%) with minimal *domed* (10–15%) distortions. The nonplanar distortion in these cocrystallates has been ascribed to intermolecular interactions/crystal packing forces.

1. Introduction

Fullerenes are of continued interest for their unique three dimensional structures and they are capable of acting as excellent electron-acceptor molecules [1–8]. Over the past three decades, there are many reports on the organic/fullerene supramolecular host–guest complexes [9,10]. The fullerene based materials are of growing attention owing to their unique physicochemical properties [11–13]. Besides, they find use in some potential material applications [14]. There are numerous reports on the fullerene-organic molecular based complexes showing varying intermolecular interactions in the solid-state. Of particular interest, the porphyrins are attractive molecular candidates to complex with the fullerenes because of their large extended π-system, tunable shape and size and they are capable of incorporating various metal ions with diverse coordination geometry and the macrocycle has stereochemical flexibility. Furthermore, the π-donor or acceptor property of the porphyrin π-system can be modulated by appending appropriate substituents at the periphery of the macrocycle [15–17].

The various electron rich porphyrin/fullerene cocrystallates have been reported in the literature [11]. Porphyrin...fullerene interaction energies as revealed from theoretical calculations showed electrostatic attractive forces that are offset by the Pauli repulsive interactions [18,19] and/or London dispersion forces [20,21]. The *meso*-tetraarylporphyrins [22–27], octaphenylporphyrin [28], octaethylporphyrin [29–31] and tetraazaporphyrazine [32] and others have been used as hosts for the cocrystallization with the fullerenes [33]. There are few reports on the use of moderately electron deficient *meso*-pentafluorophenylporphyrin as the host for the complexation with the fullerenes [26,27]. Furthermore, some dimeric [33–40], trimeric [41] and oligomeric [42–44] porphyrin were also employed as hosts for the guest fullerene cocrystallization or complexation in the condensed media. Such host–guest complexation method has been used for the separation of fullerenes [45]. The reported porphyrin/fullerene cocrystallates showed near planar geometry of the porphyrin macrocycle [22–27,33]. It is known that few tetraarylporphyrin/C_{60} cocrystallates including β-pyrrole substituted M(TPP)(Ph)$_4{\cdot}C_{60}$ (M = 2H, Co(II) and Cu(II)) cocrystallates showed nonplanar distortion of the porphyrin ring [28]. The porphyrin/fullerene cocrystallates containing electron-deficient porphyrins are largely unexplored in the literature [26,27].

In an effort to examine the influence of spherical fullerenes on the stereochemical properties of electron-deficient macrocycle and the supramolecular association between them, we have examined the cocrystallates of C_{60}/C_{70} with electron-deficient 2,3,12,13-tetracyano-5,10,15,20-tetraphenylporphyrin, $H_2TPP(CN)_4$ and its Cu(II) complex, $CuTPP(CN)_4$ and less electron-deficient 2,3,12,13-tetrabromo-5,10,15,20-tetraphenylporphyrin, H_2TPPBr_4 (Fig. 1).

* Corresponding author. Tel.: +91 44 2257 4222; fax: +91 44 2257 0509.
E-mail address: byra@iitm.ac.in (P. Bhyrappa).

http://dx.doi.org/10.1016/j.ica.2014.12.003
0020-1693/

These cocrystallates feature significant distortion of the porphyrin macrocycle. Normal-coordinate structural decomposition (NSD) analyses of the 24-atom porphyrin core for the cocrystallates revealed interesting trend in the out-of-plane distortion modes.

2. Experimental

2.1. Materials

H_2TPPBr_4, and MTPP(CN)$_4$ (M = 2H and Cu(II)) derivatives were prepared using reported procedures [46,47]. Fullerenes, C_{60} and C_{70} were procured from Sigma-Aldrich (India) were used as received. 1,1,2,2-tetrachloroethane (TCE), methanol and *n*-hexane were procured from Sigma-Aldrich (India) were of analytical grade and used as received.

The synthesised porphyrins were characterized by electronic absorption, ^{1}H NMR spectral and mass spectrometry. **H_2TPP(CN)$_4$**: UV–Vis. absorption spectrum in CH_2Cl_2: λ_{max}, nm (log ε): 439 (5.44), 449 (5.46), 553 (4.16), 599 (4.37), 687 (4.01), 728 (4.44). ^{1}H NMR ($CDCl_3$, 400 MHz) (ppm): 8.97 (s, 4H, β-pyrrole-H), 8.14 (d, 8H, *meso-o*-phenyl-H), 7.98 (t, 4H, *meso-p*-phenyl-H), 7.84 (t, 8H, *meso-m*-phenyl-H), −2.46 (s, 2H, imino-H). ESI-MS Calc. for $C_{48}H_{26}N_8$: (*m*/*z*), 715 (Calc., 714.77). **CuTPP(CN)$_4$**: UV–Vis. data in CH_2Cl_2: 439 (5.07), 541 (3.15), 638 (4.44). MALDI-MS calculated for $C_{48}H_{24}N_8Cu$: 776.30 (found: 778.50). **H_2TPPBr$_4$**: Electronic absorption spectral data in CH_2Cl_2: 436 (5.04), 534 (3.86), 614 (3.27), 683 (3.59). ^{1}H NMR ($CDCl_3$, 400 MHz) (ppm): 8.70 (s, 4H, β-pyrrole-H), 8.17 (d, 8H, *o*-phenyl-H), 7.78 (t, 12H, *m*- and *p*-phenyl-H), −2.82 (s, 2H, imino-H). ESI-MS calculated for $C_{44}H_{26}N_4Br_4$: 930.33 (found: 931.0).

3. Instrumentation

Electronic absorption spectra of porphyrins and their metal complexes were recorded on a JASCO V-550 model UV–Vis. spectrophotometer using a pair of quartz cells of 10 mm path length in CH_2Cl_2 at 298 K. ^{1}H NMR spectra of porphyrins were recorded on a Bruker Avance 400 MHz FT-NMR spectrometer in $CDCl_3$ using tetramethylsilane as the internal reference standard. Mass spectral measurements of the samples were carried out using an electrospray ionization (ESI) mass spectrometer model Micromass Q-TOF Micro with 10% formic acid in methanol/$CHCl_3$ as the solvent medium. Single crystal X-ray structure data collections were performed on a Bruker AXS Kappa Apex II CCD diffractometer with graphite monochromated Mo Kα radiation (λ = 0.71073 Å).

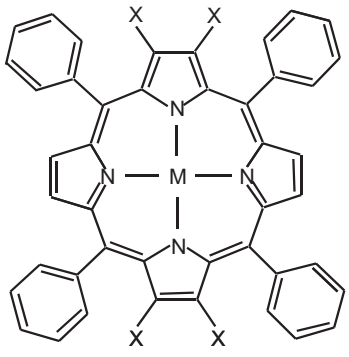

M = 2H; X = Br
M = 2H, Cu(II); X = CN

Fig. 1. Chemical structures of porphyrins and metalloporphyrins.

3.1. Crystal structures

Single crystals of $(H_2TPP(CN)_4)_3{\cdot}C_{60}{\cdot}(hexane)_{1.5}{\cdot}(TCE)_{4.83}$, **1** and $(CuTPP(CN)_4)_3{\cdot}C_{60}{\cdot}(TCE)_6{\cdot}(H_2O)_3$, **2** were grown by diffusing vapours of *n*-hexane to the equimolar quantities of porphyrin and C_{60} in 1,1,2,2-tetrachloroethane, TCE solution over a period of ten days. The crystals of $H_2TPP(CN)_4{\cdot}C_{70}{\cdot}(TCE)_6$, **3** were grown by diffusing vapours of *n*-hexane to the one-to-one stoichiometry of $H_2TPP(CN)_4/C_{70}$ in TCE solution for a period of a week. The crystals of $H_2TPPBr_4{\cdot}(C_{60})_2{\cdot}(TCE)_2$, **4** were obtained by diffusing vapours of *n*-hexane to the one-to-one equimolar concentration of porphyrin and C_{60} in saturated solution of TCE over a duration of several days. The stoichiometry of the cocrystallates obtained in the electron-deficient MTPP(CN)$_4$-to-C_{60} was found to be unaltered even by altering the stoichiometry from 1:1 to 3:1 ratios. The repeated crystallisation of **1** and **2** yielded same quality weakly diffracting crystals. The single crystals of the parent $H_2TPP(CN)_4{\cdot}(0.5\ hexane)_2$ were obtained by diffusing *n*-hexane to the saturated solution of the porphyrin in TCE over a period of four-days. Crystals were coated with inert oil and mounted to a glass fibre attached to a goniometer and cooled the crystal rapidly under the stream of liquid nitrogen of the diffractometer.

WINGX32 program was used for solving the structures by direct methods [48–50]. SHELXL-2013 software was employed to determine the non-hydrogen atoms by successive Fourier synthesis. The criterion of $F^2 > 2\sigma(F^2)$ was used for calculating R_1. All the non-hydrogen atoms were refined with anisotropic thermal parameters. Hydrogen atoms of the porphyrin structures were geometrically relocated at the chemically meaningful positions and given riding model refinement. In case of cocrystallates, **1**, **3** and **4**, the core NH hydrogens were located exclusively at the pyrroles without β-pyrrole substituents. Molecular packing diagrams and intermolecular interactions were generated using Mercury 3.3 [51] software. ORTEP diagrams of the cocrystallates were generated using ORTEP-3 for windows [52].

In case of structure, **1**, the fractional occupancy for hexane and TCE, and two disordered positions for one of the TCE solvate were observed. The cocrystallate, **2**, shows two disordered positions for one of the TCE solvate. Out of the six lattice solvates in the structure, **3**, one of the TCE shows two disordered positions whereas structure **4** feature a minor disordered bromo groups and TCE solvate. Structure **5** shows fractional occupancy of 0.5 (*n*-hexane) per half of the porphyrin unit. The disordered solvates were refined by taking sum of their occupancies to one or appropriate fractional values. The final structure solution showed unaccountable scattered residual electron density peaks in the range 1.0–1.17 e Å^{-3} in **1**, 1.0–1.90 e Å^{-3} in **2** and 1.0–1.67 e Å^{-3} in **4**. The disordered solvates were resolved using EADP, DFIX, SUMP, ISOR and DELU restraints/constraints.

4. Results and discussion

To elucidate the extent of porphyrin...C_{60} interactions, similar solvent system was employed for the crystallisation of porphyrin/C_{60} systems. Crystallographic data of all the porphyrin/fullerene cocrystallates (**1**–**4**) and the parent host $H_2TPP(CN)_4{\cdot}(0.5\ hexane)_2$ structure, **5** is also listed in Table 1. Interestingly, cocrystallization of C_{60} with MTPP(CN)$_4$ (M = 2H and Cu(II)) forms 1:3 ratio between the C_{60}-to-porphyrin. The asymmetric unit of both the cocrystallates (**1** and **2**) has one-third of C_{60} and a porphyrin unit along with the lattice solvates. Representative ORTEP of the cocrystallate **2** is shown in Fig. 2. The selected bond lengths and geometrical parameters of macrocycle in the cocrystallates are shown in Table 2. It can be seen that the observed bond lengths and angles of the porphyrin rings of **1** and **2** are comparable to